Chapter 4

Room-Temperature Fabrication of Fe_3O_4

4.1 Introduction

100% spin polarization makes the half metallic material so attractive in applications for spintronic devices. The so-called half metallic ferromagnets can provide electrons of one directional spin. Applications to spintronic devices require high Curie temperature (T_C) due to the consideration of thermal stability. Hence, the Fe_3O_4 (T_C =850K) may be superior to $LaSrMnO_3$ (T_C =360K) or CrO_2 (T_C =395K) [1-2]. Epitaxial growth of Fe_3O_4, predicted to be a half-metal, on MgO single crystal has been reported by several groups [3-5].

Rapid hoping of electron between Fe^{2+} and Fe^{3+} ions results in good room-temperature conductivity. The Verwey transition is a metal to insulator transition as the electron hopping is frozen at the temperature close to 120K (T_V：Verwey Temperature) [6]. T_V is the important characteristic of half-metallic Fe_3O_4. In published papers of Fe_3O_4 thin films, Verwey transition close to 120 K was obtained by growing films directly on single-crystal substrates at high temperature [3-5].

Gong *et al*. [3] succeeded in obtaining Ms=~415 emu/ cm^3 and T_V=~120K on a MgO(100) substrate by using a pulsed laser deposition (PLD) system, but the deposition temperature was at 350℃, and the thickness was as thick as 6600Å. Hong *et al.* [7] used a reactive rf sputtering system integrated with an external rf source to deposit Fe_3O_4

films at room temperature, the clear Verwey transition was observed at 125K. However, the M_S value of the polycrystalline films was only 190.6 emu/cm^3. Aoshima *et al.* [8] reported that the Ms of 430±50 emu/ cm^3 could be obtained on MgO (110) substrates grown at 350℃ by ion beam sputtering with a Fe_3O_4 target. However, the Verwey transition was not clearly observed. To take advantages of half-metallic films for spintronic devices, for example, TMR or GMR devices, low temperature deposition is preferred. In addition, epitaxial Fe_3O_4 films may enable us to clearly investigate the effect of the half metal without grain boundary scattering. Therefore, the main purpose of this work is to grow epitaxial Fe_3O_4 films at room temperature. We used reactive ion beam deposition (IBD) to grow Fe_3O_4.

Since the working pressure of IBD is 10^{-4} Torr, this low working pressure reduces the number of collisions between sputtered atoms and gas ions. In addition, the beam voltage of the IBD system can be independently controlled regardless of working pressure and can be raised to 1500 V. Consequently, the IBD system can provide relativity high incident energy of sputtered atoms compared to other deposition method. The energy given by the ion beam system is high enough to reduce the temperature needed for the formation of the Fe_3O_4 phase. In this work, we will discuss the magnetic, electrical and crystalline properties of Fe_3O_4 films grown on MgO (100) at room-temperature by using IBD system.

On the other hand, we should notice that if Fe_3O_4 films are applied to the electrodes of TMR junctions, a highly conductive underlayer is required because the poor conductivity of Fe_3O_4 films may lead to a

non-uniform current distribution. Furthermore, epitaxial Fe_3O_4 films may enable us to investigate the effects of the half metals on the spin transport without grain-boundary scattering. Nevertheless, the orientation of the epitaxial films is also an important issue because of various surface states. Since the (100) surface of the epitaxial Fe_3O_4 film is polar, the surface reconstruction takes place to minimize the surface energy [9]. The surface reconstruction may modify the electronic band structure and deteriorate the half-metallic characteristics. On the contrary, in the epitaxial Fe_3O_4 (111) film, a spin polarization of –(80±5) % near to the Fermi energy E_F was observed by using the spin-resolved photoemission spectroscopy [10]. Furthermore, the (111) surface is more stable and all the magnetic moments in Fe_3O_4 (111) layers lie in the film plane. On the other hand, when Fe_3O_4 films are used as electrodes in TMR junctions, a low-temperature deposition process is preferred to prevent the interdiffusion. The growth of the epitaxial Fe_3O_4 films on a conductive underlayer was reported by Kim *et al*. [11] They succeeded in obtaining T_V around 118K with an Ag underlayer on a MgO(100) substrate by using a MBE system, but their deposition temperature was 250 ℃ and the average roughness was over 30 Å. Because the IBD system can provide relatively high incident energy of sputtered atoms compared to other deposition methods, the energy given by the ion beam system is high enough to reduce the formation temperature of the Fe_3O_4 phase.

4.2 Experimental Procedures

In the first part of this chapter, Fe_3O_4 thin films were deposited at room temperature using an ion beam deposition system (IBD). The Fe_3O_4 films were prepared on Si (100) and MgO (100) substrates. The base pressure was 2×10^{-7} Torr. Pure Fe targets were used and Ar was used as processing gas. During the deposition, O_2 flow was simultaneously introduced and its flow rate was varied from 0.5 to 1.4 sccm while the flow rate of Ar was fixed at 6 sccm. The working pressure was maintained at 3×10^{-4} Torr.

In the second part of this chapter, Fe_3O_4 and Cu thin films were deposited at room temperature using an IBD system. The Cu 50 nm / Fe_3O_4 70 nm bilayers were grown on Si (001) substrates. Before depositing of Cu films, Si wafers were put into 10 % HF solution for several seconds, followed by rinsing in deionized water and drying by N_2. The accelerating voltage of the ion gun was 1000 volts, which provided a relative high energy of sputtered atoms.

Magnetic properties were measured by using Vibrating Sample Measurement (VSM) with a maximum applied field of 10 kOe. Film structures were characterized by using x-ray diffractometer. The valance state of Fe was identified by Energy Dispersive Spectrometer (EDS) and Electron Energy Loss Spectrum (EELS) attached to Transmission Electron Microscope (TEM). Electric properties were measured by using Physical Property Measurement System (PPMS). The valance state of Fe was identified by X-ray photoelectron spectroscopy (XPS). The

roughness measurement of Fe_3O_4 surface was performed by an atomic force microscopy (AFM).

4.3 Results and Discussions

4.3.a Room-Temperature Fabrication of Fe_3O_4

By accurately controlling oxygen partial pressure during deposition, a series of films with different phases, i.e., α-Fe, $Fe_{1-X}O$, and Fe_3O_4, were obtained in sequence with increasing oxygen contents, respectively.

X-ray diffraction (XRD) patterns of the 1000Å films on Si substrates with various oxygen flow rates (R_{O2}) from 0.5 to 1.4 sccm are shown in Fig 4.1. For the films deposited on Si substrates, α-Fe (110) is the only phase before introducing the oxygen gas flow; when R_{O2} is 1.0 sccm, only FeO (200) peak can be observed; when R_{O2} reaches 1.2 sccm, the phase turns to be Fe_3O_4.

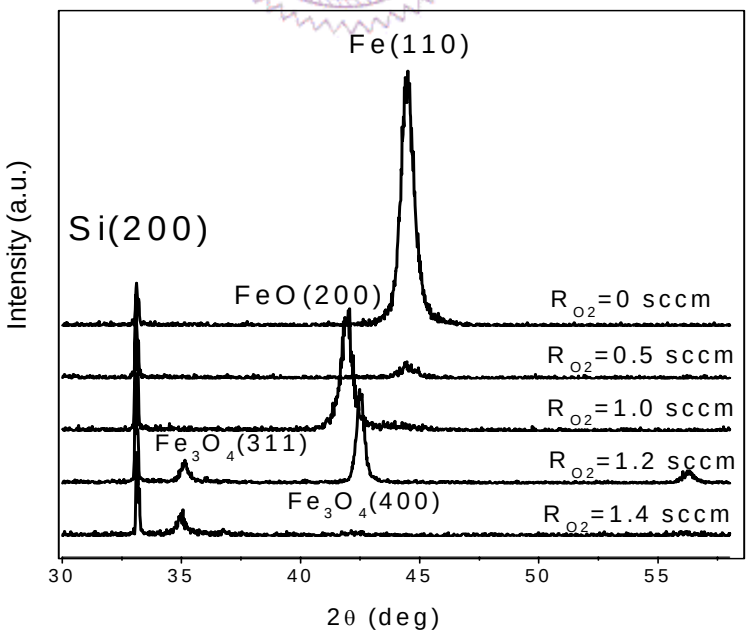

Fig. 4.1. XRD patterns of the 1000Å Fe_3O_4 films on Si substrates with various oxygen flow rates.

To analyze the valence states of Fe, EDS was performed. The determined valence states of Fe were consistent with the observed phase in XRD pattern. To further confirm the stoichiometry of the iron oxide films, we used EELS coupled with field emission gun transmission electron microscope (FEGTEM). From EELS analyses, we can characterize the 3d electron distribution of Fe. The L_3 and L_2 spectra edges of EELS spectrum are corresponding to excitation from the spin-orbit split levels $2p^{3/2}$ and $2p^{1/2}$ (initial states) to $3d^{5/2}$ and $3d^{3/2}$ (final states). The intensity ratio of L_3 and L_2 spectra edges can be used to identify the occupation number of the 3d orbital. To characterize accurately the valance state of iron oxides, double arctangent function background subtraction method was used to subtract the background noise [12]. After background subtraction, the spectrum can be fitted by two Lorentzian functions, corresponding to the L_2 and L_3 peaks, respectively. Intensity ratio of the L_2 and L_3 peaks reveals the hole numbers in d orbital that can help us to characterize the $Fe^{2+}$and Fe^{3+} in the thin films. The EELS spectrum and fitting results of Fe_3O_4 films are shown in Fig. 4.2. The calculated intensity ratio of Fe_3O_4 film is 4.14, consistent with the reported value (4.20) [13]. Based on XPS and EELS results, we can conclude that Fe_3O_4 phase can be obtained by IBD deposited at room temperature.

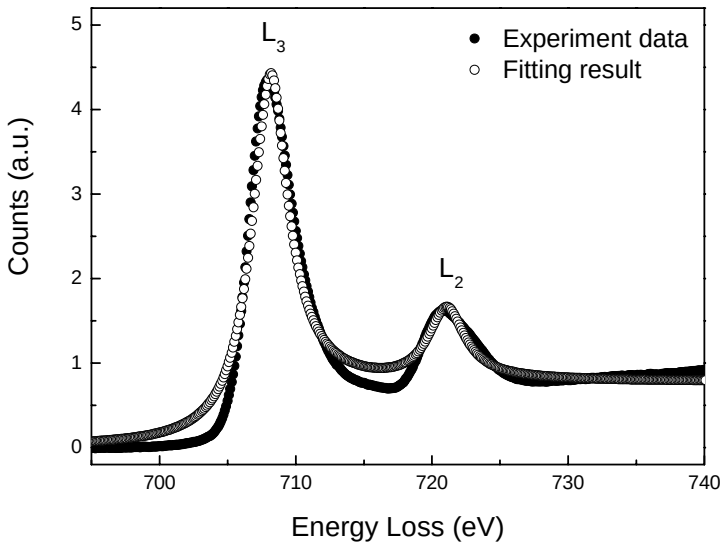

Fig. 4.2. EELS spectrum (solid circles) and fitting results (open circle) of the 1000Å Fe_3O_4 film deposited on Si substrates.

By optimizing growth conditions of Fe_3O_4 on Si (100) substrates, epitaxial Fe_3O_4 films can be obtained under the same condition on MgO (100) substrates at room temperature. Because the MgO (200) and Fe_3O_4 (400) peaks are piled up due to the equivalent distance between rows of oxygen atoms along the <100> direction, we can not distingue the Fe_3O_4 (400) peak from MgO (200) peak. However, in-plane orientation can be used to tell the orientation relationship between films and substrates. In-plane XRD φ-scans of the {311} planes, as shown in Fig. 4.3, reveal that the {311} peaks from the film aligned well with those from the substrate, confirming the epitaxial growth of Fe_3O_4 on MgO with cube-to-cube orientation relationship. This epitaxial growth can still remain for the film thickness down to 450Å. Similar results by IBD were

reported by Asohima, but its deposition temperature was at 350℃ with the Ru underlayer [8]. In addition, their Fe_3O_4 films were grown by directly sputtering on a Fe_3O_4 target, instead of reactive sputtering. Reactive sputtering seems to give more complete reaction between iron and oxygen atoms, which significantly reduces the formation temperature of the Fe_3O_4 phase. The reported room-temperature deposited Fe_3O_4 films by magnetron sputtering was also reactive sputtering [7]. However, the films were polycrystalline with a relatively low M_S value (190.6 emu/cm^3).

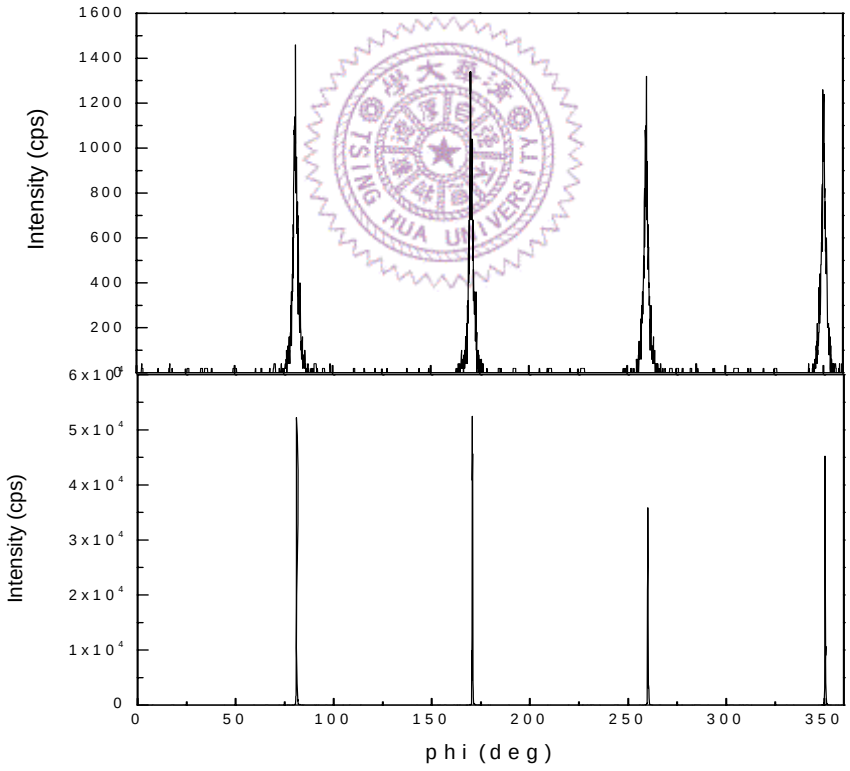

Fig. 4.3. X-ray diffraction φ-scans of Fe_3O_4 (311) peaks (upper curve), and of MgO substrate (311) peaks (lower curve).

Figure 4.4 shows the thickness dependence of the saturation moment (M_S) of the Fe_3O_4 films grown on Si (100) and MgO (100) substrates at room temperature. Ms of the films deposited on MgO is less dependent on thickness, and even when the film thickness was reduced to 45 nm; its M_S can still maintained at 301emu/cm^3. On the other hand, the M_S value of the films grown on Si decreases significantly as thickness decreases. The thickness dependence suggests that a thinner initial deal layer may be formed at Fe_3O_4/MgO interface. Epitaxial growth of Fe_3O_4 films on MgO may improve crystalline quality and reduce the dead layer. Large lattice mismatch between Fe_3O_4 films and Si substrates may induce large amount of defects or dislocation at interface. As the thickness decreases, the initial dead layer becomes dominant. The reduction of M_S value of films on MgO compared to the bulk value (~471emu/cm^3) may be attributed to slightly nonstoichiometric oxygen under room temperature growth [14].

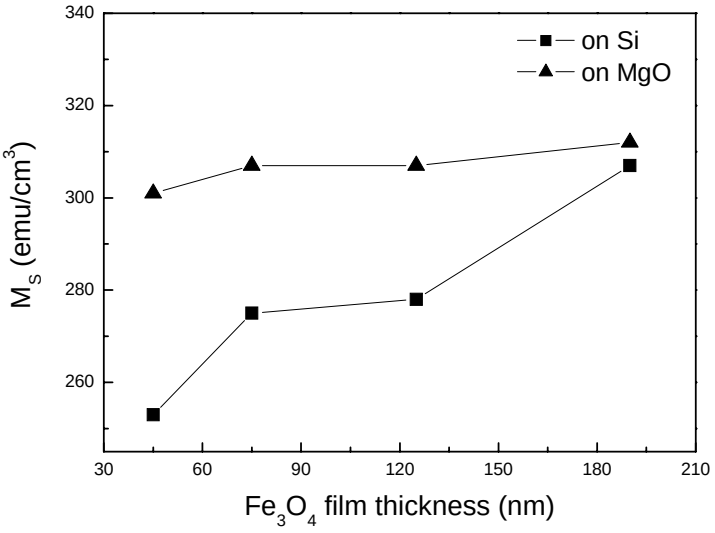

Fig. 4.4. Film thickness vs the saturation magnetization (M_S) for the Fe_3O_4 films deposited on Si and MgO substrates.

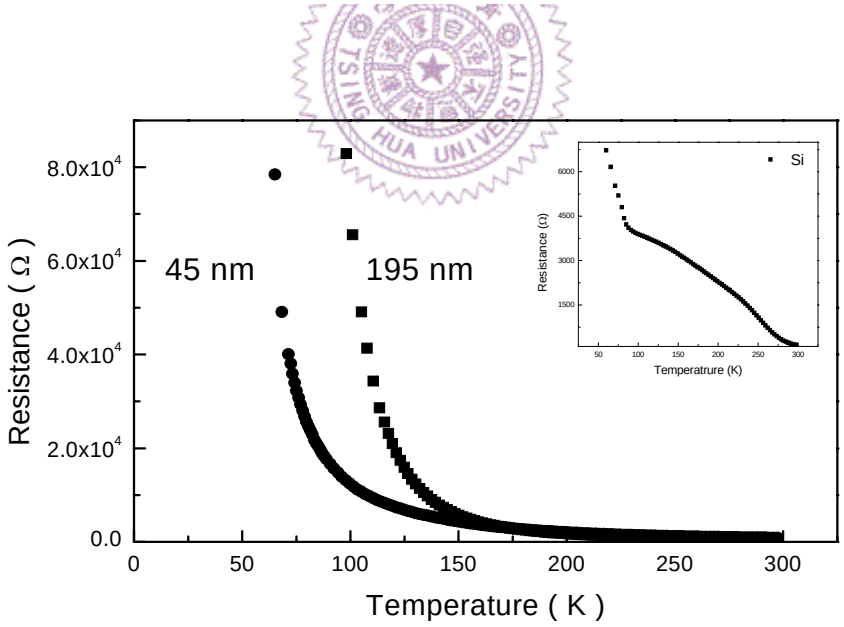

Fig. 4.5. Resistance as a function of temperature for Fe_3O_4 films grown on MgO substrates. (■:the films thickness of 195 nm; ●: 45 nm). The inset shows dependence of resistance on temperature for the 195nm Fe_3O_4 films deposited on Si substrates.

Figure 4.5 displays the resistance (R) as a function of temperature for Fe_3O_4 films on MgO (100) substrates. The resistivity value of 195nm films at room temperature is ~10000 $\mu\Omega$cm, which is consistent with Gong's reported value for his 660 nm Fe_3O_4 films by PLD system. As the temperature decrease, the resistance gradually increased, and an abrupt increase is observed around 110K. This value is little lower than the T_V value of the bulk (~121K). The slight reduction of T_V might be due to residual strain in the films resulting from the lattice mismatch with the substrates [15]. Unlike the thickness dependence of M_S, T_V dropped to 71K at film thickness of 450Å. The Verwey transition is related to the electronic structure, which may strongly depends on the equilibrium positions of atoms; therefore, residual strain in the films may significantly affect the T_V. As thickness of Fe_3O_4 films decreased, the strain effect became more pronounced; therefore, the reduction of T_V was observed. The T_V of 195 nm Fe_3O_4 films grown on Si is around 80 K, shown in the inset of Fig. 4.5, which may be attributed to less perfect crystalline quality.

4.3.b Room-Temperature Fabrication of Epitaxial Fe_3O_4 (111) Films with Conductive Underlayer

In order to avoid the non-uniform current distribution by using the Fe_3O_4 electrode, the choice of the epitaxial conductive underlayer is an important issue. An epitaxial Cu layer is a good candidate as a

conductive underlayer because its stable properties at room temperature. The XRD pattern, shown in Fig. 4.6, reveals the (200) Cu and {111} peaks of the Fe_3O_4 film, indicating a good out-of-plane (111) texture of the Fe_3O_4 film on the (200) Cu underlayer. The Cu (001) epitaxial films were reported to grow on hydrogen terminated (1×1) Si (001) reconstructed surface by metal-metal epitaxy on silicon (MMES) method [16-17]. The epitaxial relationship between Cu and Si was found to be Si (001) // Cu (001) and Si [110] // Cu [010].

In order to investigate the in-plane orientation and the epitaxial relationship between Cu and Fe_3O_4 layers, asymmetric in-plane φ-scans were performed and their results were shown in Fig. 4.7. Four {111} peaks of the Cu underlayer confirm that the Cu layer is a (001) epitaxial film. The twelve {311} peaks of the Fe_3O_4 film, shown in the Fig. 4.7, indicate an unusual 12-fold symmetry. In addition, the twelve {440} peaks appeared at the same φ values as those of the twelve {311} peaks. The {311} and {440} peaks should be separated by 60 degree in a cubic single crystal. A cubic single crystal has a 3-fold symmetry about the <111> axis. However, a 6-fold symmetry is inevitable even in high-quality (111) epitaxial films prepared by MBE [18]. This is because the epitaxial films contain twins related by a 60-degree rotation about an axis parallel to the [111] direction.

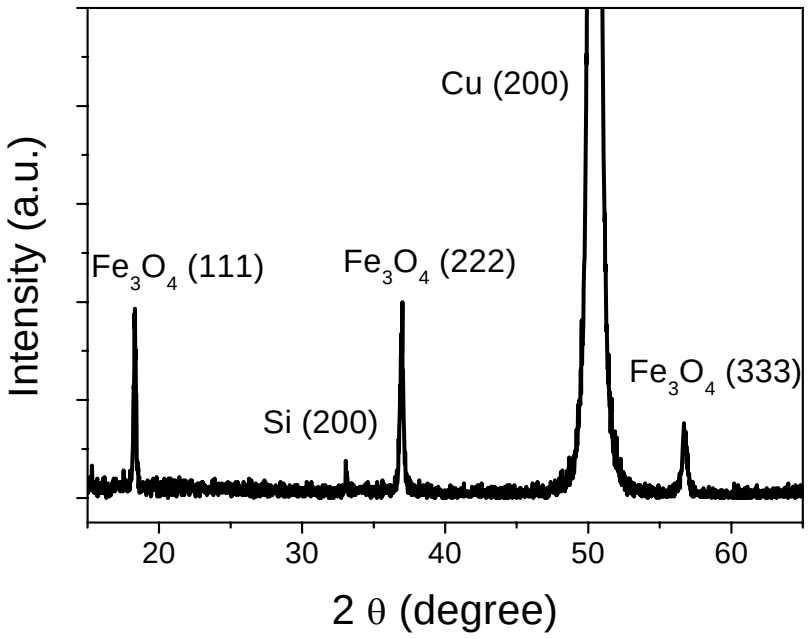

Fig. 4. 6. X-ray θ- 2θ scan of Si (001)/ Cu 50 nm / Fe_3O_4 70 nm.

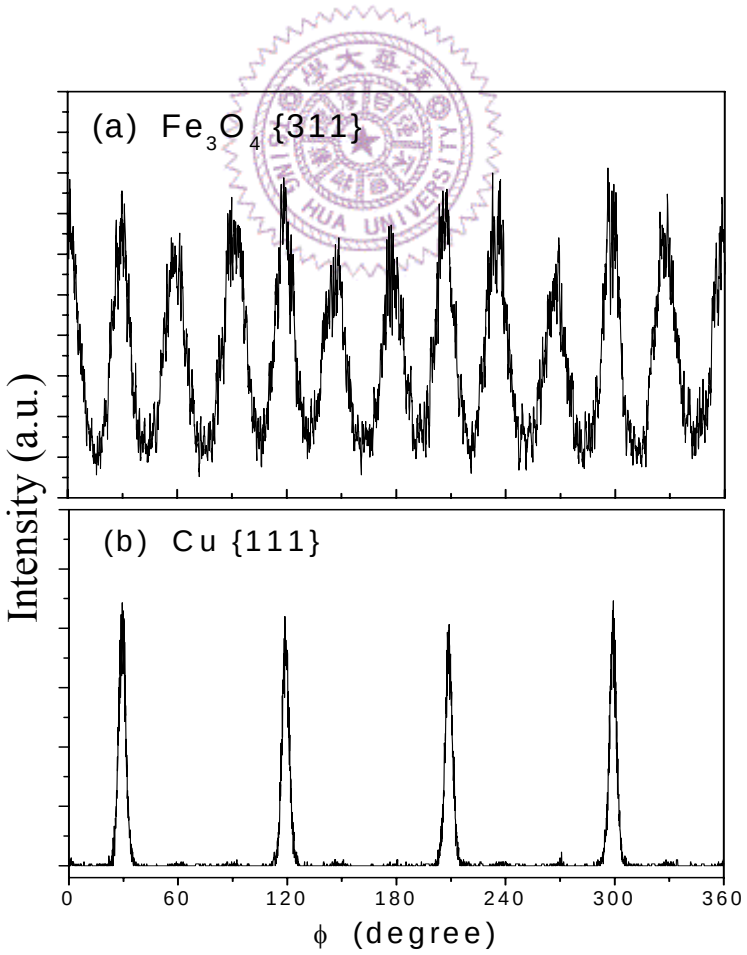

Fig. 4. 7. X-ray φ scans of (a) Fe_3O_4 {311} and (b) Cu {111}.

The twinning may result from the two equivalent stacking sequence of the {111} planes in a face-center-cubic crystal. Nevertheless, the 12-fold symmetry indicates that the in-plane orientation of Fe_3O_4 is not totally random. The selected area diffraction (SAD) patterns of Fe_3O_4 films, taken on two different grains by using the nano-beam are shown in Fig. 4.8. The direction of the electron beam is along Cu [110]. The SAD patterns of Fe_3O_4 film correspond to $[1\bar{1}2]$ and $[1\bar{1}0]$ zones. In fact, all SAD patterns taken on different grains of Fe_3O_4 revealed one of the patterns shown in Fig. 4.8, which suggested that two kinds of {111} grains existed in the Fe_3O_4 films. Two sets of the (111) epitaxial grains (marked as "A" grain and "B" grain) rotated by 90 degree with respect to each other along [111] direction. The results from XRD and TEM diffraction enable us to determinate the orientation relationships between the Cu and Fe_3O_4 layers, as shown in Fig. 4.8 (c). The orientation relationships are: Fe_3O_4 (111) // Cu (001), Fe_3O_4 $[1\bar{1}2]$ // Cu $[\bar{1}10]$, Fe_3O_4 $[1\bar{1}0]$ // Cu [110] in "A" grain and Fe_3O_4 (111) // Cu (001), Fe_3O_4 $[11\bar{2}]$ // Cu [110], Fe_3O_4 $[\bar{1}10]$ // Cu $[\bar{1}10]$ in "B" grain. Reactive sputtering and high incident energy provided by IBD seem to give more complete reaction between iron and oxygen atoms, which significantly reduces the formation temperature of the Fe_3O_4 phase. Furthermore, the structural template provided by the (001) Cu underlayer helps the sputtered atoms to move into the lattice sites of Fe_3O_4 at room temperature.

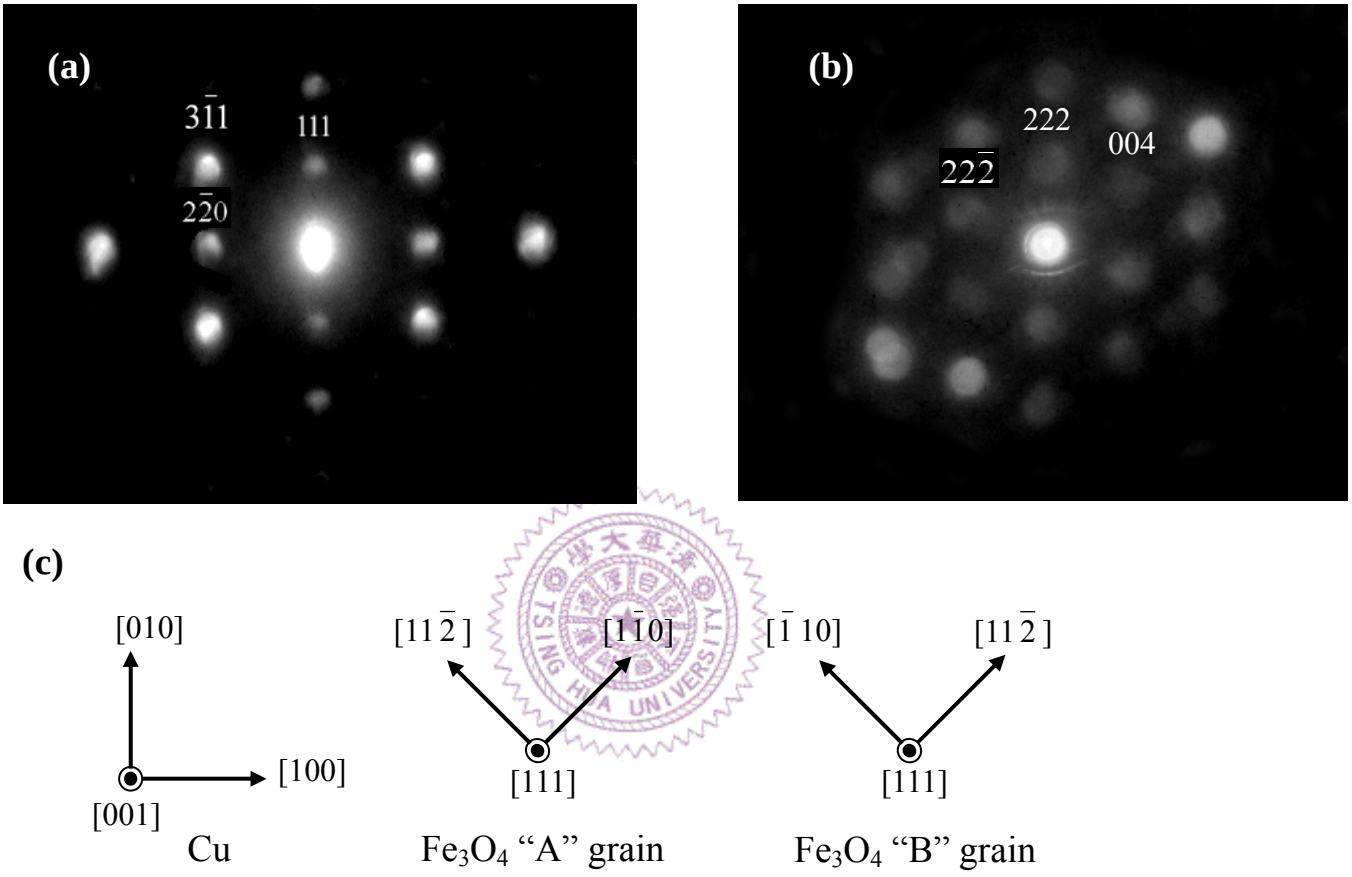

Fig. 4.8. SAD patterns of Fe_3O_4 films on (a) "A" grains ([11$\bar{2}$] zone) and (b) "B" grains ([1$\bar{1}$0] zone). The direction of electron beam is along Cu [110]. (c) The schematic diagram of the orientation relationship between Cu (001) and Fe_3O_4 (111).

Although the structure of the Fe_3O_4 was well characterized, it is worthy to notice that the γ-Fe_2O_3 (maghemite) has the same cubic structure (inverse spinel) and similar lattice constants (a= 0.835 nm) to the Fe_3O_4 (a= 0.839 nm). It is quite challenging to only use XRD patterns to conclusively exclude the existence of γ- Fe_2O_3 in the film. To verify the phases, X-ray photoelectron spectroscopy (XPS) was performed to analyze the chemical states of Fe. Fig. 4.9 shows the Fe 2p core-level photoemission spectrum of the Fe_3O_4 film taken at hν = 1486.6 eV. Due to spin–orbit coupling, the Fe 2*p* core levels split into $2p^{3/2}$ and $2p^{1/2}$ peaks that are located at about 711 and 724 eV, respectively. Furthermore, the Fe $2p^{3/2}$ main peaks of the Fe^{2+} and Fe^{3+} components have binding energies of 709 eV and 711 eV, respectively. Therefore, the broadening of the Fe $2p^{3/2}$ main peak in Fig. 4.9 indicates the coexistence of Fe^{2+} and Fe^{3+}. The absence of the satellite peak situated at about 719 eV, which is the characteristic of Fe^{3+} in γ - Fe_2O_3, suggests that γ - Fe_2O_3 does not exist in the films [19].

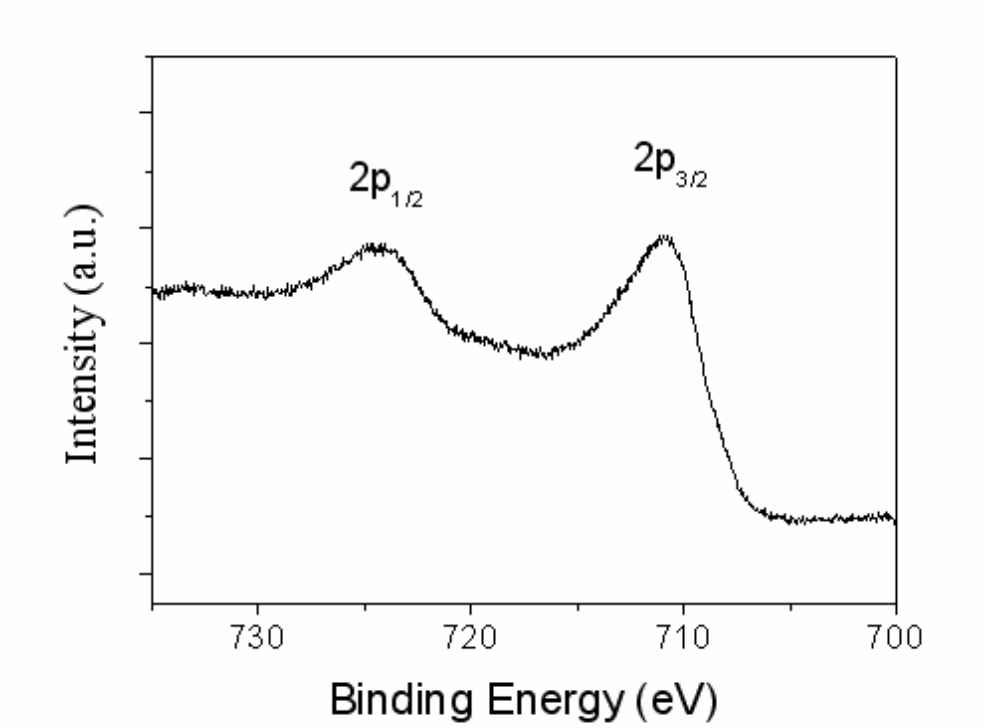

Fig.4.9. XPS spectrum of 70 nm thick Fe_3O_4 film on Cu underlayer taken at $h\nu$ = 1486.6 eV.

As mentioned in the pervious section, T_V is the important characteristic of stoichiometric Fe_3O_4. The magnetic and electric transport properties of Fe_3O_4 are sensitive to the stoichiometry. In addition, because of the shunting effect of the Cu underlayer, the transport data was difficult to exclude the contribution from Cu layer when the CIP measurement was performed. Therefore, we measured the temperature dependence of magnetic moment of Cu/Fe3O4 bilayer in this section. When Fe_3O_4 is cooled through the T_V in a small magnetic field, a sharp decrease in the magnetization is observed [20]. At room temperature, the saturation magnetization M_S of 70 nm thick (111) Fe_3O_4 films is 291 emu / cm^3 with

a maximum applied field of 10 kOe. Fig. 4.10 displays the dependence of magnetization (M) on temperature of the 70 nm Fe_3O_4 film on epitaxial Cu underlayer, measured in a constant field of 100 Oe. Because the applied field is only 100 Oe, the substrate effect can be neglected. As the temperature decreased, the magnetization was gradually increased, and an abrupt decrease was observed around 116K. This value is similar to the T_V value of the bulk (~121K), which indicates the formation of stoichiometric Fe_3O_4 films. The decrease of magnetization with temperature below T_V is not as sharp as the result reported may be partially associated with the distribution of the orientations(two kinds of grains) in our Fe_3O_4 films. In addition, the strain existing in Fe_3O_4 films grown on Cu may also result in the gradual change of M vs. T, as Margulies reported [5].

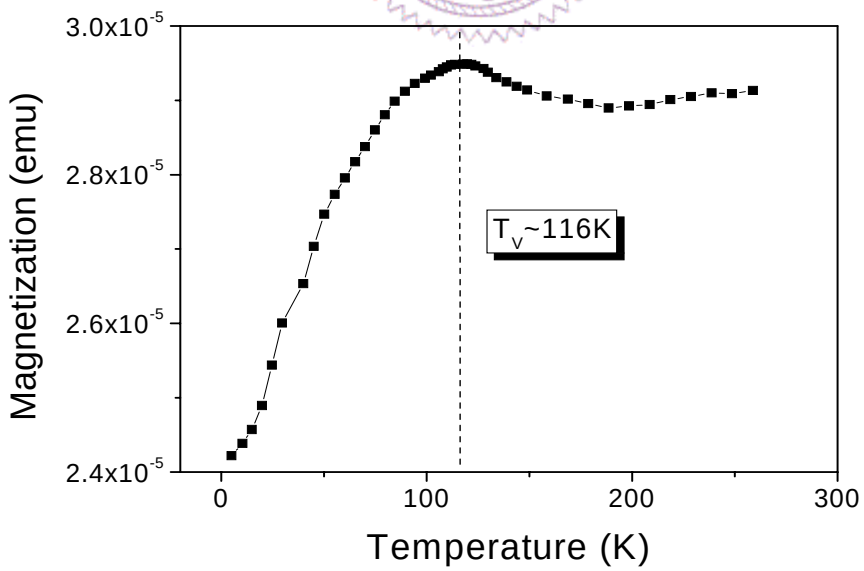

Fig.4.10. Temperature dependence of magnetization of 70 nm Fe_3O_4 films on epitaxial Cu underlayers, measured at a constant field of 100 Oe.

Interface roughness is an important issue for fabricating high quality TMR junctions. The root-mean-square (r. m. s.) roughness of the 70 nm Fe_3O_4 film on the Cu underlayer is only 3.5 Å, much smoother than that deposited on the MgO or α-Al_2O_3 substrates [11]. The TMR junctions composed of this epitaxial (111) Fe_3O_4 films and Al_2O_3 barrier layers showed relatively low TMR values (<10 %) [8]. The selection of suitable barrier materials may be critical to fully utilize the half-metal characteristics of Fe_3O_4 films.

4.4 Summary

By accurately controlling oxygen partial pressure during deposition, polycrystalline and epitaxial Fe_3O_4 films can be grown at room temperature by reactive ion beam deposition on Si (100) and MgO (100) substrates, respectively. EELS and XRD analyses suggested that the Fe_3O_4 phase can be obtained at room temperature by the relatively high incident energy provided by the IBD system. Epitaxial (100) Fe_3O_4 films showed less thickness dependence of M_S than polycrystalline ones, which might suggested that a thinner initial dead layer was formed on MgO due to epitaxial growth. In addition, the T_V of 110K was observed on 195 nm epitaxial (100) Fe_3O_4 films, and significantly decreased with decreasing thickness. The reduction of T_V in thin films may be related to the effects of residual strain.

The high-quality epitaxial Cu/ Fe_3O_4 films deposited at room-temperature were obtained by using reactive ion beam sputtering. X-ray φ-scans revealed unusual 12-fold symmetry of (111) Fe_3O_4 films on Cu (001) underlayers. TEM diffractions verified that the two sets of the (111) epitaxial grains rotated by 90 degree with respect to each other along [111] direction were formed in the Fe_3O_4 layer. A clear Verwey transition observed at 116K indicates the formation of a stoichiometric Fe_3O_4 film. The r. m. s. roughness of the Fe_3O_4 surface is only 3.5Å.